Mon. Not. R. Astron. Soc. **260,** 915–924 (1993)

Reddening and age for 11 Galactic open clusters from integrated spectra★

João F. C. Santos, Jr and Eduardo Bica
Instituto de Física-UFRGS, Porto Alegre, RS, Brazil

Accepted 1992 August 18. Received 1992 August 18; in original form 1992 April 23

ABSTRACT

We study integrated spectra of 11 Galactic open clusters in the visible and near-infrared. We use continuum distribution and line strengths to infer reddening, age and, in some cases, metallicity. These parameters are derived by using different methods, mainly by employing template integrated spectra of Magellanic Clouds and Galactic star clusters with known properties, as well as a grid relating the equivalent widths of spectral absorption lines to age and metallicity spanning a wide range of values. The results indicate a good agreement with previous work based mainly on colour–magnitude diagrams, when available. Internal reddening is significant for very young clusters like NGC 3603 and 6611. A Wolf–Rayet star in NGC 6231 is also analysed spectroscopically in the cluster context. Wolf–Rayet features appearing in the integrated spectra of NGC 6231 and 3603 are employed as indicators of the cluster evolutionary stage. The oldest cluster in the sample has an age ≈ 300 Myr. The present sample considerably improves the age resolution around solar metallicity in the cluster spectral library for population synthesis.

Key words: stars: abundances – stars: evolution – stars: Wolf–Rayet – dust, extinction – open clusters and associations: general.

1 INTRODUCTION

The study of the integrated spectra of star clusters is a fundamental link between stellar population studies of galaxies and stars. This can help to clarify important questions such as the chemical evolution and formation of galaxies (see e.g. Pagel & Edmunds 1981; Frogel 1988).

Reddening, age and metallicity determinations for Galactic open clusters have been mostly based on colour–magnitude diagrams (CMDs) and observations of individual stars (Hagen 1970; Janes 1979; Mermilliod 1981; Battinelli & Capuzzo-Dolcetta 1991 and references therein). Integrated spectra can provide similar information, e.g. Bica & Alloin (1986a, hereafter BA86a). Galactic open clusters are fundamental as calibrators of integrated properties in view of population synthesis studies in galaxies and the determination of astrophysical parameters of star clusters in distant galaxies for which it is not possible to obtain CMDs. Galactic open clusters have, in general, large angular sizes and low concentrations of stars. However, some of them are still suitable for integrated spectrum observations (BA86a).

In the present work we increase considerably the sample of Galactic open clusters with integrated spectroscopy. We aim to determine the astrophysical parameters of the clusters by means of, amongst other methods, the grid of metallic and Balmer-line equivalent widths as a function of age and metallicity in Bica & Alloin (1986b, hereafter BA86b). The 11 new integrated spectra of the clusters will also be useful for future extragalactic studies, when incorporated into the existing library.

The observations and measurements are presented in Section 2. In Section 3 we explain the methods for deriving age, reddening and metallicity. A discussion of individual clusters is provided in Section 4. The Wolf–Rayet (W-R) features in NGC 3603 and 6231 are analysed as age indicators in Section 5. Additional applications of the cluster integrated spectra are presented in Section 6 and the final conclusions are in Section 7.

2 THE DATA

2.1 Observations

We have selected concentrated, relatively populous Galactic open clusters to allow good star sampling in the integrated spectrum. The 11 clusters and the log of observations are presented in Table 1. All the integrated spectra were

★Based on data collected at the European Southern Observatory, La Silla, Chile and at the Laboratório Nacional de Astrofísica/CNPq Brazil.

Table 1. Observations.

Cluster	Date	UT	Exposure Time (min.)	Airmass
NGC3603 cl.	5/24/90	0:23	15	1.19
neb.	5/24/90	0:45	5	1.23
NGC4755	7/5/88	22:15	18	1.31
	7/10/88	23:23	28	1.42
NGC5617	7/5/88	23:27	40	1.29
	7/12/88	22:38	45	1.28
	7/13/88	23:10	30	1.30
	7/14/88	0:00	30	1.36
NGC5999	5/22/90	6:31	20	1.23
	5/22/90	7:34	10	1.29
NGC6067	7/9/88	0:58	48	1.19
	7/9/88	2:00	48	1.27
	7/10/88	1:47	54	1.27
NGC6231 cl.	7/6/88	23:42	30	1.10
	7/7/88	0:23	30	1.07
	7/8/88	1:47	18	1.08
	7/9/88	3:50	28	1.36
W-R	7/8/88	1:30	5	1.07
	7/9/88	4:51	4	1.70
	7/9/88	5:00	4	1.77
NGC6520	5/23/90	6:09	20	1.01
NGC6603	5/23/90	5:06	15	1.05
	5/23/90	5:41	15	1.11
NGC6611 cl.	7/9/88	3:42	40	1.09
	7/12/88	4:00	42	1.15
neb.	7/9/88	4:45	18	1.26
NGC6756	5/21/90	7:48	20	1.21
Mel105	5/24/90	1:57	20	1.31

Note. In the first column the entries cl., neb. and W-R stand respectively for cluster, nebular gas associated with the cluster, and a Wolf–Rayet star associated with the cluster. When nothing is indicated, the global cluster was observed.

obtained by scanning the slit across the cluster. The spectrophotometry carried out in 1988 July was made with an OMAIII detector, a 4×20 or 30 arcsec^2 slit and a 300 line/mm grating at the 0.6-m telescope of the Laboratório Nacional de Astrofísica (LNA), Itajubá, Brazil. The average resolution, as obtained from comparison-lamp spectra, was 20 Å in the spectral range $4700 < \lambda < 8800$ Å. The signal-to-noise ratio (S/N) was typically 15. The standard stars observed were HR 5501, 7596, 7950 and 9087. The observations in 1990 May were obtained with the 1.52-m telescope at the European Southern Observatory (ESO), La Silla, Chile. We employed the RCA CCD ESO # 13 detector (readout window: 300×1024 pixel^2) coupled to a Boller & Chivens spectrograph with grating ESO # 13. The slit size covered 1.5 arcsec $\times$ 3.6 arcmin on the sky. The average resolution achieved was 15 Å over the range $3800 < \lambda < 8800$ Å, with typical S/N around 30. The standard stars observed in this run were LTT 3218, LTT 7987 and EG 274. The reduction procedure used was the standard one using the IRAF (1988 run) and IHAP (1990 run) softwares. For the LNA observations the sky background was scanned away from the cluster in separate exposures; the long-slit ESO observations used sky background in the same exposure frame or a separate one, depending on the cluster angular size. Most objects were observed at least twice to test the sampling and reproducibility. The relative fluxes of a given cluster for the LNA spectra are within 20 per cent, whereas the ESO ones are within 10 per cent.

Table 2. Equivalent widths for (a) the ESO clusters and (b) the LNA clusters.

(a)

Window $\lambda_o/\Delta\lambda$ ident.	3603	5999	Cluster 6520	NGC 6603	6756	Mel105
3838/48 H9	0.4	9.2	5.8	8.1	12.6	8.0
3885/46 H8	1.2	5.2	5.4	10.2	9.0	8.3
3930/44 KCaII	0.5	2.7	3.0	2.5	1.8	2.3
3970/36 HCaII+H_ϵ	1.6	8.1	7.7	9.4	9.6	10.1
4103/42 H_δ	1.3	9.8	7.4	11.4	11.7	10.7
4182/64 CN	2.5	2.7	3.2	0.4	1.8	2.7
4229/30 CaI	1.1	0.8	1.5	0.6	0.3	0.4
4301/34 CH	1.8	2.0	3.5	1.3	2.0	2.4
4341/46 H_γ	2.7	8.7	8.7	12.4	8.9	11.0
4865/38 H_β	-0.5	9.9	6.6	11.8	9.7	9.6
5176/40 MgI+MgH	0.1	4.1	2.3	2.0	0.9	1.3
5279/70 FeI	-0.1	1.9	2.0	2.2	1.0	1.3
5897/34 NaI	3.1	-0.1	1.8	3.3	2.7	2.3
6563/46 H_α	-19.9	6.0	2.6	3.8	6.2	6.4
7257/414 TiO	-20.8	8.6	9.6	24.7	10.4	14.7
8197/74 NaI	-4.1	6.1	2.2	2.3	1.5	3.9
8498/44 CaII+P16	1.3	4.2	4.8	7.0	6.3	5.3
8542/44 CaII+P15	2.0	5.8	6.5	4.7	4.6	5.2
8670/60 CaII+P13	1.6	5.4	5.1	6.6	7.3	8.0

(b)

Window $\lambda_o/\Delta\lambda$ ident.	4755	Cluster 5617	NGC 6067	6231	6611
4865/38 H_β	2.4	4.1	6.6	1.4	-10.8
5176/40 MgI+MgH	0.5	0.7	1.5	0.5	-1.1
5279/70 FeI	0.9	2.4	0.6	0.2	0.1
5897/34 NaI	1.6	2.1	1.7	0.1	3.0
6563/46 H_α	0.2	3.4	4.5	-3.3	-125.0
7257/414 TiO	36.0	24.4	31.1	3.6	15.2
8197/74 NaI	10.6	4.4	6.8	7.2	9.5
8498/44 CaII+P16	3.5	1.6	2.2	0.6	4.3
8542/44 CaII+P15	4.7	8.3	6.0	1.6	3.2
8670/60 CaII+P13	5.0	8.3	1.4	2.7	6.5

Note to Table 2. Equivalent widths are in ångström units and were obtained following window definitions from Bica & Alloin (1986a, 1987). Negative values indicate emission. In the first column we provide the central wavelength and the window width as well as the main contribution absorbers. The errors are less than 5 per cent in the visible and less than 20 per cent in the near-infrared.

2.2 Measurements

The equivalent widths in spectral windows as defined by BA86a and Bica & Alloin (1987, hereafter BA87) were calculated for our cluster sample using the spectral analysis program SPEED and the results are presented in Tables 2(a) for ESO/CCD observations and 2(b) for LNA/OMA observations. Estimated errors are <5 per cent in the visible and <20 per cent in the near-infrared. The continuum tracings are according to BA86a, BA87 and Bica & Alloin (1988). The contamination by residual interference fringes is mainly responsible for the larger error in the latter spectral range. The equivalent widths are in ångström units (Å) and negative values indicate emission.

Table 3. Equivalent widths for Wolf–Rayet features.

Window $\lambda_o/\Delta\lambda$ ident.	Cluster 6231	NGC 3603
4633/40 NIl	-	4.1
4620/110 CIII+HeII	40.3	-
4699/40 HeII	-	9.3
5560/46 OV	0.3	-
5690/65 CIII	13.8	-
5819/20 CIV	-	0.6
5824/69 CIV+HeII	22.4	-
6555/81 HeII+H_α	6.6	25.9
6731/95 CIII	7.8	-
7051/82 HeI	2.9	-
7125/47 NIV	-	5.3
7727/72 CIV	4.6	-

Note. The nebular gas present in NGC 3603 accounts for a significant contribution of Hα to the emission around 6563 Å, in contrast to NGC 6231 whose main contributor is the Wolf–Rayet He II feature.

The equivalent widths for the W-R features identified in the integrated spectra of NGC 3603 and 6231 are given in Table 3.

3 AGE, REDDENING AND METALLICITY ESTIMATES

Equivalent widths of H Balmer lines and the near-infrared Ca II triplet are direct indicators of age and metallicity respectively (e.g. BA86a, BA87). Simultaneous estimates of age and reddening can be obtained by comparing the continuum (and lines) of programme cluster spectra to those of template cluster spectra with known parameters. The Balmer decrement is employed for clusters with gas emission in order to derive reddening. The occurrence of W-R stars is used as an additional criterion for age ranking for the associated cluster.

The template cluster spectra are those in Bica (1988). They are average spectra of Magellanic Clouds (MC) and Galactic clusters grouped according to their evolutionary stages. The groups that were useful in the present analysis are Y1 (age $t \approx 10$ Myr), Y2 ($t \approx 50$ Myr), Y3A and Y3B ($t \approx 100$ Myr) and Y4 ($t \approx 500$ Myr). The Y1 group corresponds to the red supergiant phase, and Y3B has an enhanced population of massive asymptotic giant branch stars with respect to Y3A (BA86a). Further MC cluster spectra and finer classification groups were also studied in the near-infrared by Bica, Alloin & Santos (1990); in the present study, blue spectra of the LMC clusters NGC 2003 and 1767 ($t \approx 7$ Myr) were used as templates for the evolutionary stage intermediate between H II regions and the Y1 group. These spectra, taken at the 1-m telescope of Cerro Tololo with the 2D Frutti detector, were reduced in a standard way. We also used as template NGC 2070 (30 Dor) for the H II region phase. This template (BA86a) is a combined spectrum of the stellar content and gas emission such as to reproduce the Hβ equivalent width as observed through a large diaphragm (Dottori & Bica 1981). The template sequence is essentially one-parameter, age being the parameter. The metallicity plays a secondary role in the visible/ultraviolet ranges because the templates consist of young blue clusters, where the abundance effects on the continuum distribution are negligible.

In Sections 3.1–3.4 we explain in detail the methods employed to derive age, reddening and metallicity for the cluster sample. The results are given in Tables 4 and 5.

Table 4. Age determination for the sample (Myr).

Cluster NGC	Template match	W(Balmer)	Literature	(Source)
3603	2	-	2.5±2	MTT89
4755	8.5	<10	10	DK84
			12	M81
5617	50	34±20	46	BC91
5999	100	230±170	-	
6067	50	79±18	78	M81
			150	TWH62
6231	4.5	-	6.2	M81
			3.2	BC91
			7.9±3	PHC91
6520	50	56±16	800	S66
6603	100	200±120	-	
6611	2	-	5	SJ79
			4	TWFW90
6756	300	400±90	-	
Mel105	100	250±150	100	FDK89

Note. Columns 2 and 3 show the ages obtained from the template match and from the Balmer-line equivalent width, respectively. Column 4 refers to the age derived from the photometric studies in column 5. References: MTT89 = Melnick et al. 1989; DK84 = Dachs & Kaiser 1984; M81 = Mermilliod 1981; BC91 = Battinelli & Capuzzo-Dolcetta 1991; TWH62 = Thackeray et al. 1962; PHC91 = Perry et al. 1991; S66 = Svolopoulos 1966; SJ79 = Sagar & Joshi 1979; TWFW90 = Thé et al. 1990; FDK89 = Frandsen et al. 1989.

Table 5. $E(B-V)$ determination for the sample.

Cluster NGC	Template	Literature	(Source)
3603	1.18±0.02	1.48	MTT89
		1.37	BF71
4755	0.4±0.1	0.35	M81
		0.31	BF71
		0.41	DK84
5617	0.3±0.1	0.53	BC91
		0.51	BF71
5999	0.44±0.02	-	
6067	0.10±0.05	0.37	BF71
		0.35	M81
		0.30	TWH62
6231	0.25±0.05	0.41	BF71
		0.48	M81
		0.46	BC91
		0.44	PHC91
6520	0.56±0.02	0.27	S66
6603	0.50±0.02	0.47	BF71
6611	0.3±0.1	0.74	BF71
		0.78	SJ79
		0.90	TWFW90
6756	0.7±0.1	1.26	BF71
Mel105	0.30±0.02	0.38	FDK89

Note. Column 2 refers to the template match method, while column 3 gives reddenings obtained by means of photometry as referenced in column 4. Abbreviations as in Table 4, except for BF71 (= Becker & Fenkart 1971).

3.1 Age from Balmer lines and W-R features

A direct age estimate was obtained from equivalent widths of the Balmer lines in absorption in each spectrum (Table 2). We interpolated these values in the age calibration of BA86b (their table II). The ages derived by this method are reddening-independent. We also analysed the presence of W-R stars in two clusters (NGC 6231 and 3603) as a characteristic of their evolutionary phases (Section 5).

3.2 Age/reddening by template match

This method consists of matching a cluster spectrum to that of the template which most resembles it. As a first guess for the template we use the reddening-independent ages provided by the previous method. Then reddening and template are varied to get the best match of continuum and lines. Results are illustrated for different clusters in Fig. 1.

Only foreground reddening has been applied to the templates and, consequently, if a determination of total (foreground + internal) reddening is available, it is then possible to estimate the internal reddening due to dust within the cluster (Section 4). It is also important to consider the possibility of a significant differential internal reddening, especially for the youngest clusters.

3.3 Reddening from emission lines

The Balmer decrement was also employed to derive reddening for the youngest clusters with substantial gas content, NGC 6611 and 3603. The theoretical flux ratio $F(\mathrm{H}\alpha)/F(\mathrm{H}\beta)=2.87$ and the extinction curve in Osterbrock (1989) were adopted.

3.4 Metallicity

The equivalent widths for the Ca II triplet at 8498, 8542 and 8662 Å (Table 2) are average values of the high- and low-continuum tracings in BA87. The latter tracing minimizes the TiO and H Paschen contaminations. In cases of emission contamination and/or low S/N it was not possible to determine metallicity. The values were interpolated in table A3 of BA87 to provide the metallicity estimates in Section 4.

4 DISCUSSION OF INDIVIDUAL CLUSTERS

In this section we discuss the results obtained for each cluster.

4.1 NGC 3603

The ionizing cluster associated with the NGC 3603 complex is very frequently compared to that of NGC 2070 (30 Dor) in the LMC: both are rich clusters with central objects of a similar nature and are embedded in giant H II regions (e.g., Moffat & Niemela 1984; Melnick, Tapia & Terlevich 1989). The parameters derived for NGC 3603, together with results from other authors, are summarized in Tables 4 and 5. We have determined simultaneously the age and reddening for this cluster (Section 3.2) by using as a template the integrated spectrum of the cluster associated with 30 Dor (NGC 2070) of age 2.0 ± 0.5 Myr (BA86a and references therein). We recall that the MC templates are not corrected for internal reddening and consequently the template match provides the foreground reddening $E(B-V)_{\mathrm{f}}$. The best match gives $E(B-V)_{\mathrm{f}}=1.18\pm0.05$ for NGC 3603. Fig. 2 shows the cluster integrated spectrum corrected for this reddening value, where we have identified some features. An independent reddening estimate was derived from the Balmer

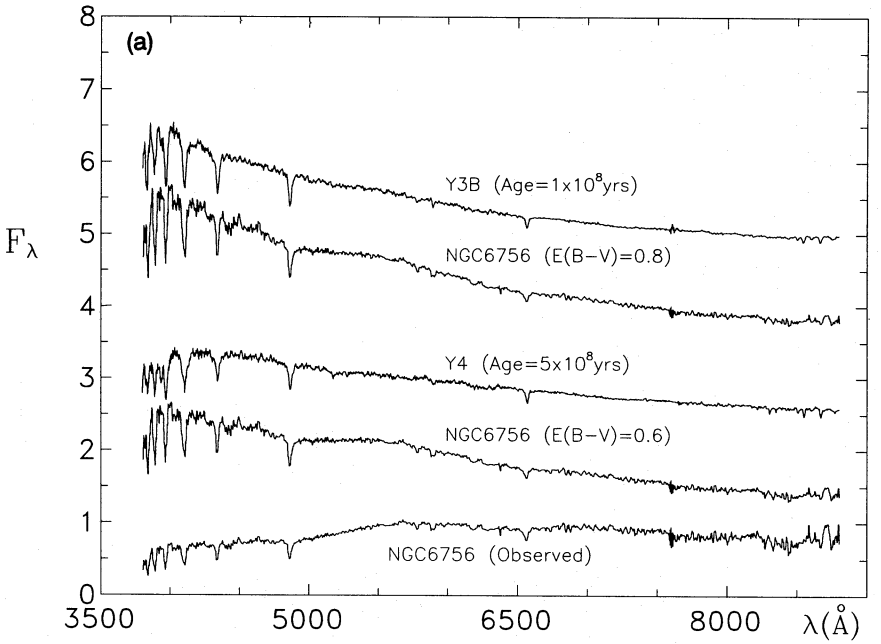

Figure 1. Examples of template spectrum match. We show the observed cluster spectrum, the same corrected for a derived foreground reddening value and the template which best matches the spectrum. (a) NGC 6756, where we also show an alternative match; (b) NGC 6520; (c) Mel 105. The spectra are normalized at 5870 Å. We used relative F_λ units, shifted by a constant when necessary.

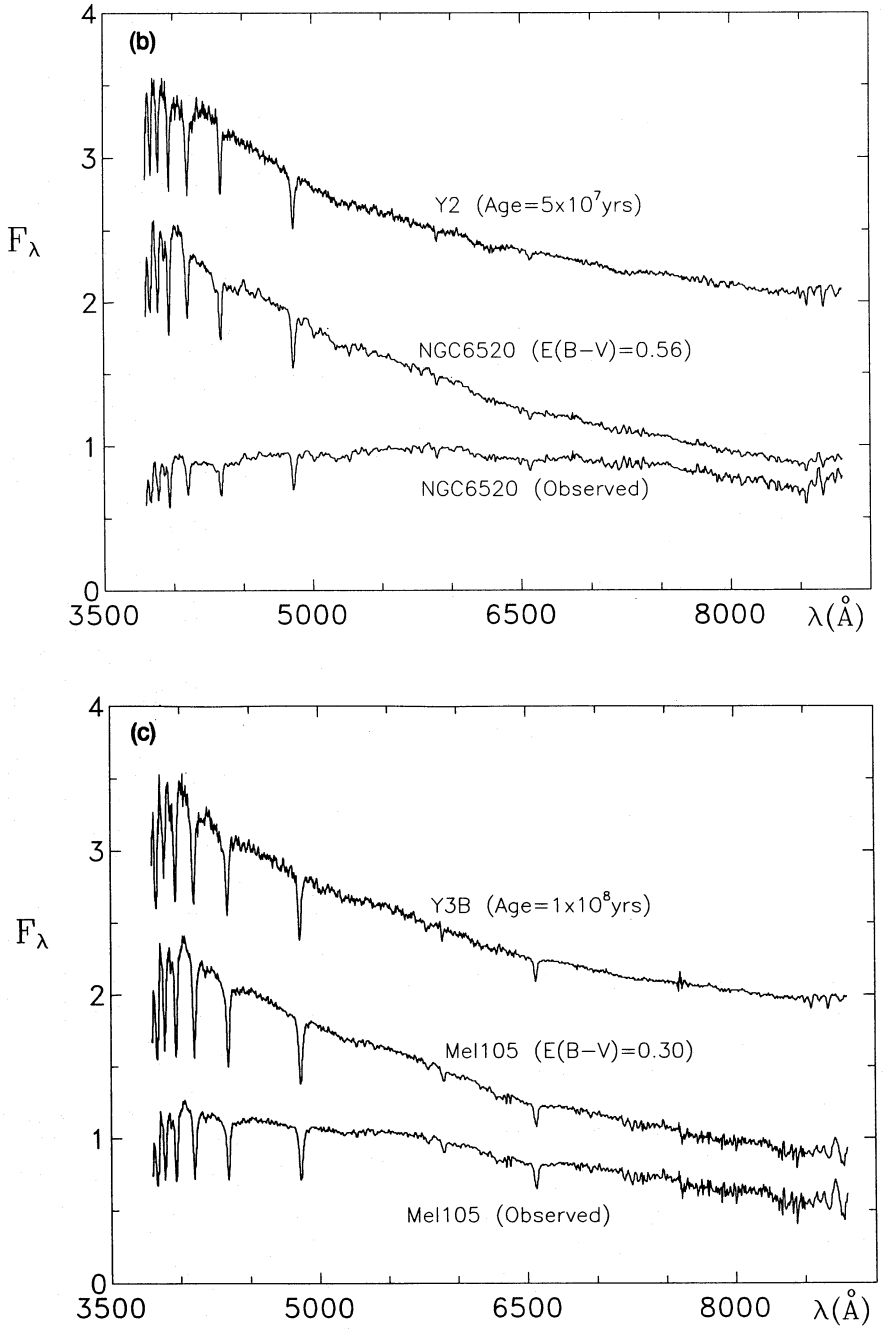

Figure 1 – *continued*

emission line decrement: the gas filament spectrum (Table 1) gives a total (foreground + internal) reddening $E(B-V)_t = 1.51$. The difference between these two methods furnishes an estimate of the internal reddening $E(B-V)_i = 0.33$, at least in the direction of the gas filament observed.

The ratio $F(\mathrm{H}\alpha)/F(\mathrm{H}\beta)$ in emission measured in the star cluster integrated spectrum yields a misleadingly high value of $E(B-V)_t = 2.17$. It is an expected result because the stellar content absorbs part of emission in the Balmer line wavelengths, the absorption of Hβ being stronger than that of Hα in the integrated light of a young star cluster (BA86a).

The spectral characteristics of NGC 3603 match very well those of NGC 2070, in particular the WN features, and consequently the derived age 2.0 ± 0.5 Myr is a fiducial estimate. Our results are compatible with those of Melnick et al. (1989), who derived an age of 2.5 Myr with a real spread of 2 Myr. They obtained an average total reddening $\langle E(B-V)_t \rangle = 1.44$ with $\sigma = 0.13$ from the member stars within a radius of 50 arcsec. Their total reddening compares well with ours derived from the gas filament. In Section 5 we discuss the W-R component of NGC 3603 as additional information about the cluster evolutionary stage.

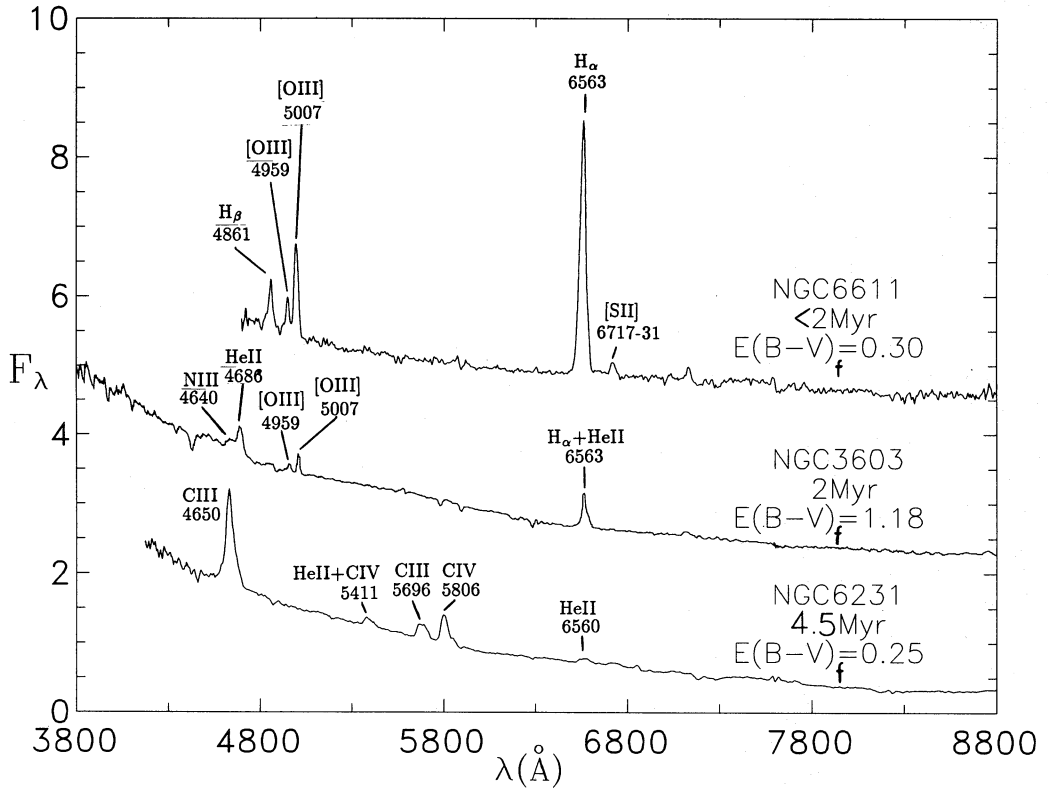

Figure 2. The integrated spectra of NGC 6611, 3603 and 6231 are presented. Some features characteristic of W-R and gas components are identified. The spectra are ranked in age.

4.2 NGC 4755 = κ Crucis

The best continuum match for this cluster is NGC 1767 (7 Myr), but NGC 4755 has stronger TiO bands (see Table 2b), very similar to those in the Y1 template (10 Myr). This suggests that the cluster is close to or within the red supergiant phase. Indeed, one red star in the cluster centre was classified as having spectral type M2Iab (Mermilliod 1976 and references therein). Our average age (8.5 Myr) is in good agreement with those in the literature (Table 4). The reddening resulting from the match $E(B-V)_f = 0.4 \pm 0.1$ is compatible with the results of other authors (Table 5). The weakness of Balmer absorption lines in the integrated spectrum indicates $t < 10$ Myr. Ca II triplet equivalent widths give $[Z/Z_\odot] = -0.18 \pm 0.16$.

4.3 NGC 5617

The best match is for the Y2 template (50 Myr) with reddening $E(B-V)_f = 0.3 \pm 0.1$. The age obtained by means of the equivalent width of H Balmer lines (34 ± 20 Myr) supports the age estimated from the Y2 template and is in agreement with that presented by Battinelli & Capuzzo-Dolcetta (1991) (see Table 4). The comparison with other works based on CMDs (Table 5) shows that the internal reddening produced within NGC 5617 is $E(B-V)_i = 0.2$.

4.4 NGC 5999

The solution for this cluster provides an age of 100 Myr and $E(B-V)_f = 0.44$ by template match. The age from Balmer lines is slightly greater (Table 4). No photometric study of this cluster is available for comparison. The derived metallicity is $[Z/Z_\odot] = 0.18 \pm 0.04$.

4.5 NGC 6067

A review of photometric studies on NGC 6067 has been presented by Mermilliod at al. (1987). Thackeray et al. (1962) obtained the cluster age on the basis of the spectral type of the earliest stars on the main sequence. This appears to be an overestimate when one compares it with the age calculated from the age–period relation applied to the Cepheid V340 Nor, a very probable cluster member. As pointed out by Mermilliod, Mayor & Burki (1987), a cluster including Cepheids must be between 50 and 100 Myr old, a narrow age range. Specifically, NGC 6067 falls in the 78-Myr Pleiades age group of Mermilliod (1981), which is compatible with our results from the template method (50 Myr) or the Balmer lines (79 ± 18 Myr). From the difference between the template-match foreground reddening and the literature average (excepting Thackeray's low value), we get $E(B-V)_i = 0.26$ for the internal reddening, slightly larger than that of NGC 5617. The metallicity of $[Z/Z_\odot] = -0.22 \pm 0.56$ has been derived and is comparable to that given by Janes (1979), i.e. $[Z/Z_\odot] = -0.13 \pm 0.07$.

4.6 NGC 6231

Like NGC 3603, this cluster presents W-R features, but they are of WC type (Fig. 2). The clusters also differ in the sense that the intracluster and close surrounding medium in

NGC 3603 still contains strong interstellar gas emission. NGC 6231 is embedded in an extended system of O and early-B stars, the Sco OB1 association. Sco OB1 contains the ring-shaped H II region IC 4678, centred on NGC 6231 and particularly bright away from the cluster at the northern edge of the association. NGC 6231 has been confirmed as the nucleus of Sco OB1 (Perry, Hill & Christodoulou 1991). Two templates were compared to NGC 6231 because the cluster properties are intermediate between NGC 2070 (gas-rich) and NGC 2003 (gas-free). The average age derived is 4.5 Myr, in good agreement with other methods (Table 4). The average reddening $[E(B-V)_f = 0.25 \pm 0.05]$ combined with the CMD-derived total reddening in the literature $[E(B-V)_t = 0.45 \pm 0.04$; see Table 5] suggests internal dust with $E(B-V)_i = 0.20 \pm 0.06$. Further discussion of the WC features is given in Section 5.

4.7 NGC 6520

The *RGU* photometry carried out by Svolopoulos (1966) indicated an age of 800 Myr and a reddening of $E(B-V)_t = 0.27$, both in disagreement with our results from integrated spectroscopy: a stronger reddening $[E(B-V)_f = 0.56 \pm 0.02]$ and a low age (around 50 Myr) provide the best solution in the present work (see Fig. 1b). The computed metallicity is $[Z/Z_\odot] = 0.38 \pm 0.16$.

4.8 NGC 6603

The best template match is $E(B-V)_f = 0.50 \pm 0.02$ for an age of 100 Myr. The age from the Balmer lines is 200 ± 120 Myr. Only one reddening estimate is available in the literature, $E(B-V)_t = 0.47$ (Table 5), which suggests that internal reddening is negligible. The spectral properties of this cluster are very similar to those of NGC 5999.

4.9 NGC 6611 = M 16

This cluster is embedded in a strong emission nebula, with dark and bright patches, a signature of very recent star formation. The 30 Dor template provides $E(B-V)_f = 0.3 \pm 0.1$ for NGC 6611. Fig. 2 presents the cluster spectrum corrected for this value. The pure emission filament (Table 1) gives $E(B-V)_t = 1.12$. Thus an internal reddening $E(B-V)_i = 0.82$ is inferred, compatible with the occurrence of dense dust clouds in the H II region. The evolutionary stage of this object is discussed in Section 5.

4.10 NGC 6756

We show in Fig. 1(a) two template matches. The template match with Y3b (100 Myr) gives $E(B-V)_f = 0.8 \pm 0.1$, whereas Y4 (500 Myr) gives $E(B-V)_f = 0.6 \pm 0.1$. A detailed inspection of the spectra reveals that the 4000-Å break is absent in NGC 6756, which favours Y3b as a match. The Balmer-line method gives an age closer to Y4 (Table 4). The only CMD study available (Svolopoulos 1965) leads to an exceedingly high reddening (Table 5), and consequently no reliable estimate for the internal reddening could be derived. It is important to obtain new photometric observations to clarify this point.

4.11 MEL 105

The cluster spectrum is shown in Fig. 1(c). The match provides an age similar to those of NGC 5999 and 6603. The reddening derived in the match combined with the CMD total reddening from the literature (Table 5) indicates an internal reddening $E(B-V)_i = 0.08$.

5 W-R STARS AS AGE INDICATORS

W-R stars are generally associated with late phases of massive-star evolution in which a high mass-loss rate (10^{-5}–10^{-4} $M_\odot$ yr^{-1}) is occurring. This mass loss removes the outer layers of the star and exposes its core. He-burning is going on in the star core (Maeder 1990a). Due to the very short evolution time of W-R stars, the presence of this type of star in clusters like NGC 3603 and 6231 can be used to date them. Spectroscopically, the W-R stars are divided into two types: WN, in which emission lines of N dominate, and WC, in which emission lines of C and O dominate. An evolutionary scenario has been proposed for the Galactic W-R subtypes based on observational grounds: intermediate and late WN stars evolve into intermediate WC stars for galactocentric distances $R > 6.5$ kpc and into late WC stars for $R < 8.5$ kpc; early subtype WN stars do not evolve into WC stars (van der Hucht et al. 1988 and references therein).

At nearly solar metallicity, the minimal initial mass M_i for a star to become a W-R is 25 $M_\odot$ (Maeder 1990a). Maeder (1990b) provided massive-star evolution models in which specific mass-loss rates are adopted for the W-R observed phases: $\dot{M}_{WR} = 4 \times 10^{-5}$ $M_\odot$ yr^{-1} for WNL stars (WN with H present) and $\dot{M}_{WR} = (0.6\text{–}1.0) \times 10^{-7} (M_{WR}/M_\odot)^{2.5}$ $M_\odot$ yr^{-1} for WNE (WN with no H present) and WC (products of partial He-burning visible) stars. These models indicate that, at solar metallicity, the larger the progenitor mass, the larger the W-R lifetime. The evolution time from the zero-age main sequence (ZAMS) to the end of the W-R phase for a solar metallicity star of 25 $M_\odot$ is 7.7 Myr, while for one of 120 $M_\odot$ it is 3.5 Myr (Maeder 1990b). Thus 7.7 Myr is an upper limit for the age of clusters that contain W-R stars. Maeder's models indicate that the W-R lifetime is 0.1 Myr for $M_i = 25$ $M_\odot$ and 1.2 Myr for $M_i = 120$ $M_\odot$. Consequently, we can observe W-R stars within solar metallicity clusters with ages in the range from 7.6 to 7.7 Myr in the case of $M_i = 25$ $M_\odot$ and in the range from 2.3 to 3.5 Myr in the case of $M_i = 120$ $M_\odot$. Fig. 3 shows the lifetime of W-R stars for various progenitor masses following Maeder (1990b). The diagram allows one to determine, in a consistent way, the age of clusters containing W-R star(s) by adopting Maeder models. If one knows the present mass and the subtype of a W-R star, then one is able to recognize the progenitor mass from which it evolved, thereby establishing its lifetime and consequently an age range for the associated cluster.

Two W-R stars have been associated with NGC 6231: WR 78 (HD 151932) and WR 79 (HD 152270), the former being located ≈ 30 arcmin away from the cluster centre, while the latter is near the centre and was included in the integrated spectrum of NGC 6231. WR 79 was also observed individually (Table 1) and in its spectrum we have identified and calculated equivalent widths for the main

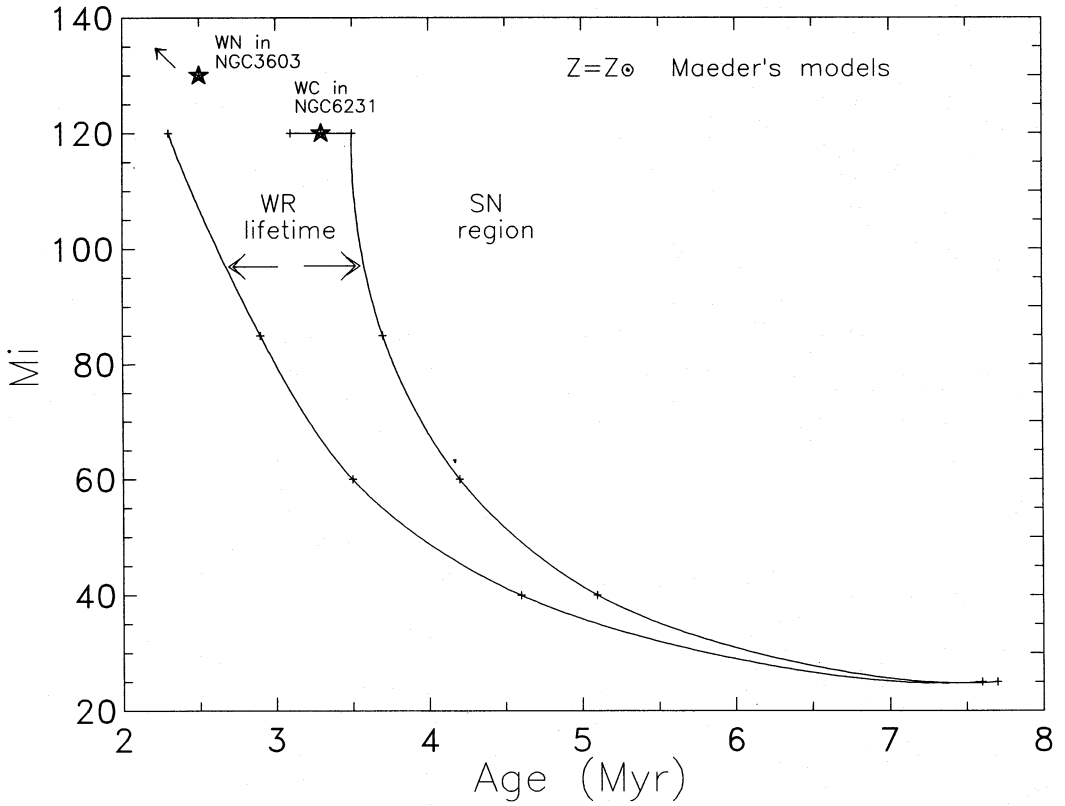

Figure 3. The W-R lifetime as a function of the progenitor mass according to Maeder's models for solar metallicity. This allows one to infer the ages of clusters that contain W-R stars. The loci of the W-Rs in NGC 3603 and 6231 are shown.

features. These data confirm the classification by Smith, Shara & Moffat (1990), i.e. WR 79 is of type WC7. The star forms a spectroscopic binary system with an O5–8 star, which allowed the determination of the present mass of WR 79, 5 ± 2 $M_\odot$ (St-Louis et al. 1987). Maeder's model of initial mass 120 $M_\odot$ and $Z = Z_\odot$ is compatible with the observations of the W-R in NGC 6231. Indeed, this model predicts a stellar mass of 5 ± 2 $M_\odot$ in the WC evolutionary phase 3.3 ± 0.2 Myr, close to our estimated cluster age of 4.5 Myr (Table 4). The mass-loss rate at this WC stage in the model is 5×10^{-6} $M_\odot$ yr^{-1}. According to this model, we are observing the star WR 79 very close to its final fate. Up until now the star has lost 96 per cent of its mass. However, we must recall that WR 79 is member of a binary system, and mass exchange may have modified the evolution from that of a single star, for which the models apply.

Moffat & Niemela (1984) have studied the core of NGC 3603 (HD 97950, WR 43), concluding that about three W-R stars of similar subclass (WN6) exist there. In addition, they pointed out that other H II regions also present similar characteristics: the η Car nebula with three WN7 stars and 30 Dor with about 15 W-R stars, most of which are WN6–7. There are two reasons to believe that the progenitors for WN6 stars observed in NGC 3603 were more massive than 120 $M_\odot$: (1) The estimated age for this cluster, 2.0 ± 0.5 Myr (Table 4), does not fully fit the WN age range in the 120-$M_\odot$ Maeder model, although some superimposition occurs. (2) It has been calculated from binary-system studies that the masses of WN6 stars should stay between 20 and 43 $M_\odot$ (van der Hucht et al. 1988). In the 120-$M_\odot$ model this mass range corresponds to the transition WN–WC, or an age around 2.8 Myr. Even if we look for other metallicities lower or higher than solar, we are not able to reproduce the observations by using models of $M_i \leq 120$ $M_\odot$. We show in Fig. 3 the locus of the W-Rs in NGC 3603 and 6231 in the initial mass-versus-age diagram.

The integrated spectrum of NGC 6611 shows gas emission lines superimposed on an OB-type spectrum (Fig. 2). Unfortunately, the observed spectral range for NGC 6611 does not reach the 4640/4686-Å WN features. However, the gas emission lines are stronger in NGC 6611 than in NGC 3603, which suggests that the former is very probably the youngest cluster in our sample. The simultaneous presence of gas with weaker lines and WN6 stars in NGC 3603 indicates a step forward in time evolution. The next step should look like NGC 6231: a cluster free of gas and with a WC7 star, in agreement with the aforementioned evolutionary scenario for W-R stars. It is important to point out that this scenario may not apply everywhere, because particular situations and phenomena must be considered in order to encompass deviations from this picture. For example, we must take into account the possibility of the simultaneous presence of WN and WC stars in the same cluster (if its star formation lasted sufficiently long) and the physical properties of the molecular cloud from which the cluster formed. More integrated spectra of clusters at such ages are necessary to get insight about cluster evolutionary states.

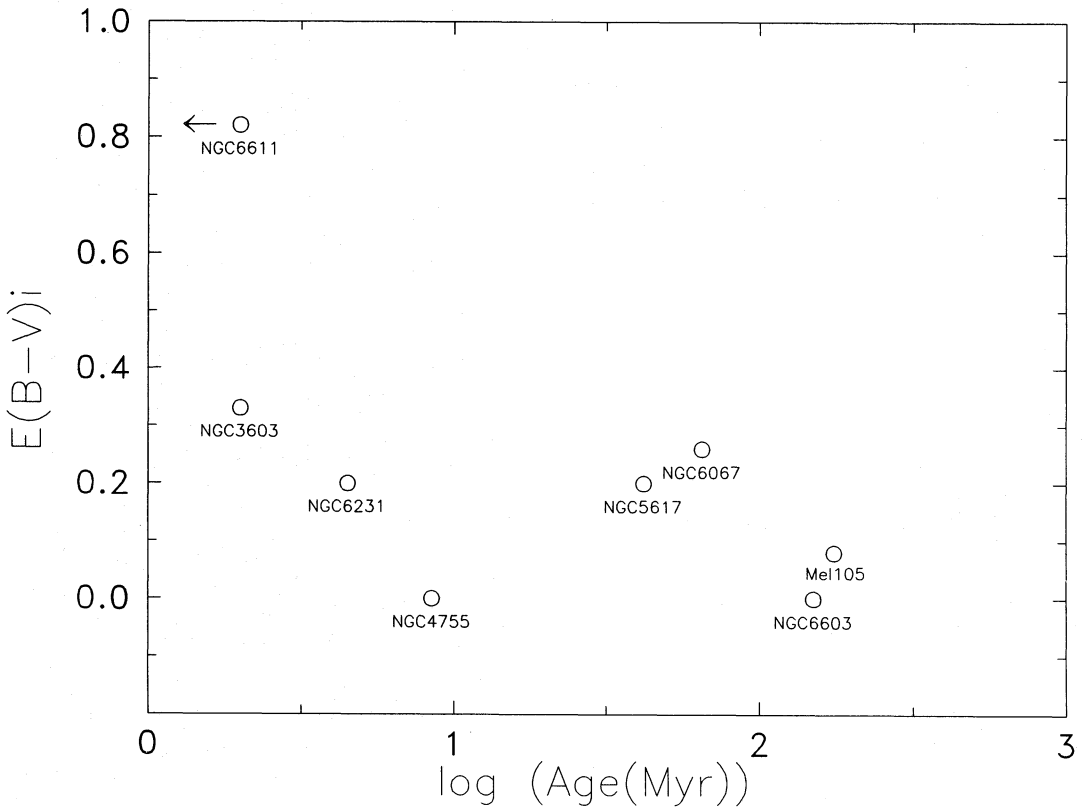

Figure 4. Internal reddening as a function of log(age).

Table 6. Age groups.

Age (Myr)	Components	E(B-V)$_i$
<2	NGC6611	0.82
2	NGC3603	0.33
4.5	NGC6231	0.20
8.5	NGC4755	0
50	NGC5617, NGC6067, NGC6520*	0.23
150	NGC5999*, NGC6603, Mel105	0.04
350	NGC6756*	-

Note. The internal reddening and age attributed to each group are average values for the member clusters. An asterisk on a cluster name indicates that itnernal reddening was not estimated because CMD information is uncertain or lacking.

6 ADDITIONAL APPLICATIONS OF THE CLUSTER SPECTRA

We show in Fig. 4 the internal reddening derived in Section 4 as a function of cluster age. This figure suggests that the internal dust dissipates in about 100 Myr.

In Table 6 we present the cluster sample grouped according to age as discussed in Section 4. We also provide in this table the average internal reddening associated with each group. These groups increase considerably the age resolution of the existing spectral library, for blue clusters of solar metallicity. This is important for the application of synthesis techniques in two ways: (i) as base elements in spectral syntheses of galaxies (Bica 1988); (ii) as objects to be synthesized with stellar libraries (Santos, Bica & Dottori 1990). In particular, the stellar population of galaxies presenting W-R features can be analysed by including in the base of clusters those with WN and WC stars.

Table 3 shows that the equivalent width of the He II (4686 Å) W-R feature in the spectrum of NGC 3603 is 9.3 Å, deblended from the N III (4640 Å) feature by means of a Gaussian deconvolution. The value is comparable to that we have calculated in the NGC 2070 (30 Dor) spectrum, i.e. 10.2 Å. Measurements by D'Odorico, Rosa & Wampler (1983) of 23 extragalactic giant H II regions give values always less than 10 Å. This suggests that, in NGC 3603 and 2070, we are looking at the peak flux contribution of W-R stars in a single generation of star formation.

7 CONCLUSIONS

We have classified the integrated spectra of Galactic open clusters according to their evolutionary phase in order to improve the existing star-cluster library used for population synthesis of galaxies. We have estimated ages, foreground and internal reddening, and metallicities in some cases. In particular, the youngest clusters in our sample are at different evolutionary stages as indicated by the presence of W-R features and nebular emission in their spectra. This can be used to disentangle age components in galaxies which are close in evolutionary stage to those characterized by the WN and WC stars. The internal reddening results in Galactic open clusters suggest that most of the dust dissipates in 100 Myr.

ACKNOWLEDGMENTS

This work has been partially supported by the Brazilian institution CNPq. We thank Roberto Cid Fernandes, Jr for help in the observing run in 1988 July, Charles Bonatto for making available his Gaussian fitting program, Alex Schmidt for his spectral analysis program SPEED and Horacio Dottori for helpful discussions on W-R stars.

REFERENCES

Battinelli P., Capuzzo-Dolcetta R., 1991, MNRAS, 249, 76
Becker W., Fenkart R., 1971, A&AS, 4, 241
Bica E., 1988, A&A, 195, 76
Bica E., Alloin D., 1986a, A&A, 162, 21 (BA86a)
Bica E., Alloin D., 1986b, A&AS, 66, 21 (BA86b)
Bica E., Alloin D., 1987, A&A, 186, 49 (BA87)
Bica E., Alloin D., 1988, in Kron R. G., Renzini A., eds, Towards Understanding Galaxies at Large Redshifts. Kluwer, Dordrecht, p. 77
Bica E., Alloin D., Santos J. F. C., Jr, 1990, A&A, 235, 103
Dachs J., Kaiser D., 1984, A&AS, 58, 411
D'Odorico S., Rosa M., Wampler E. J., 1983, A&AS, 53, 97
Dottori H., Bica E., 1981, A&A, 102, 245
Frandsen S., Dreyer P., Kjeldsen H., 1989, A&A, 215, 287
Frogel J., 1988, ARA&A, 26, 51
Hagen G. L., 1970, An Atlas of Open Cluster Colour–Magnitude Diagrams, Publ. of the David Dunlop Observatory, University of Toronto
Janes K. A., 1979, ApJS, 39, 135
Maeder A., 1990a, in Leitherer C. et al., eds, Review of Massive Stars in Starbursts, STScI Workshop, Baltimore. Cambridge Univ. Press, p. 97
Maeder A., 1990b, A&AS, 84, 139
Melnick J., Tapia M., Terlevich R., 1989, A&A, 213, 89
Mermilliod J. C., 1976, A&AS, 24, 159
Mermilliod J. C., 1981, A&A, 97, 235
Mermilliod J. C., Mayor M., Burki G., 1987, A&AS, 70, 389
Moffat A. F. J., Niemela V. S., 1984, ApJ, 284, 631
Osterbrock D. E., 1989, Astrophysics of Gaseous Nebulae. Freeman, San Francisco
Pagel B., Edmunds M., 1981, ARA&A, 19, 77
Perry C. L., Hill G., Christodoulou D. M., 1991, A&AS, 90, 195
Sagar R., Joshi U. C., 1979, Ap&SS, 66, 3
Santos J. F. C., Jr, Bica E., Dottori H., 1990, PASP, 102, 454
Smith L. F., Shara M. M., Moffat A. F. J., 1990, ApJ, 358, 229
St-Louis N., Drissen L., Moffat A. F. J., Bastien P., Tapia S., 1987, ApJ, 322, 870
Svolopoulos S. N., 1965, Z. Astrophys., 61, 105
Svolopoulos S. N., 1966, Z. Astrophys., 64, 67
Thackeray A. D., Wesselink A. J., Harding G. A., 1962, MNRAS, 124, 445
Thé P. S., de Winter D., Feinstein A., Westerlund B. E., 1990, A&AS, 82, 319
van der Hucht K. A., Hidayat B., Admiranto A. G., Supelli K. R., Doom C., 1988, A&A, 199, 217